Manuscript Details

Manuscript number ATP_2018_90

Title On the relationship between filament eruptions and solar energetic particles

Abstract

In the current study the association rate between solar energetic particles (protons) and filaments and/or filament eruptions (FEs) is investigated using a larger event sample than previously. Proton events observed in the period 2010 − 2016 are accompanied by filaments in 53% (82/156) of the cases. Due to the lack of comprehensive catalog of all filaments, a catalog of FE is used for the reversed association. Only about 5% of FEs have in situ proton signatures of larger median intensity, compared to the median of the entire proton sample. Other eruptive phenomena (flares and coronal mass ejections) related to the proton events show differences in their distributions compared to the respective FE-samples. The indication for a shock wave formation using the type II radio signatures is also considered and discussed.

Submission Files Included in this PDF

File Name [File Type]

highlights.doc [Highlights]

Tsvetkov, Miteva, Petrov.pdf [Manuscript File]

allSEPs.eps [Figure]

Fig1.eps [Figure]

Fig1a.eps [Figure]

Fig1b.eps [Figure]

Fig3a.eps [Figure]

Fig3b.eps [Figure]

Fig5a.eps [Figure]

Fig5b.eps [Figure]

Fig6b.eps [Figure]

SnSEPn.eps [Figure]

Fig6a.eps [Figure]

SEPwithEPwithoutAR.eps [Figure]

Submission Files Not Included in this PDF

File Name [File Type]

mybibfile.bib [LaTeX Source File]

Tsvetkov, Miteva, Petrov.tex [LaTeX Source File]

To view all the submission files, including those not included in the PDF, click on the manuscript title on your EVISE Homepage, then click 'Download zip file'.

Research Data Related to this Submission

There are no linked research data sets for this submission. The following reason is given:
Data will be made available on request

- Filament-related proton events are slightly more common than non-related (53/47 %).
- The majority of the proton events originate from the western hemisphere (≈70 %).
- 87% of solar energetic particle-related filaments are localized in active regions.
- Only 5% of the eruptive filaments tend to produce proton events.

On the relationship between filament eruptions and solar energetic particles

Ts. Tsvetkov[a,*], R. Miteva[b], N. Petrov[a]

[a] Institute of Astronomy and National Astronomical Observatory, Bulgarian Academy of Sciences, 72 Tsarigradsko Chaussee Blvd. 1784 Sofia, Bulgaria

[b] Space Research and Technology Institute, Bulgarian Academy of Sciences, Acad. G. Bonchev Str., 1113 Sofia, Bulgaria

Abstract

In the current study the association rate between solar energetic particles (protons) and filaments and/or filament eruptions (FEs) is investigated using a larger event sample than previously. Proton events observed in the period 2010−2016 are accompanied by filaments in 53% (82/156) of the cases. Due to the lack of comprehensive catalog of all filaments, a catalog of FE is used for the reversed association. Only about 5% of FEs have in situ proton signatures of larger median intensity, compared to the median of the entire proton sample. Other eruptive phenomena (flares and coronal mass ejections) related to the proton events show differences in their distributions compared to the respective FE-samples. The indication for a shock wave formation using the type II radio signatures is also considered and discussed.

Keywords:
solar activity, filaments, energetic particles, protons

1. Introduction

For more than a century now, the different aspects of solar activity are considered to be undoubtedly connected. All of them owe their existence to the magnetic field and represent different ways in which solar plasma

*Corresponding author
Email address: tstsvetkov@astro.bas.bg (Ts. Tsvetkov)

is responding to the underlying magnetic field evolution [1]. Solar eruptions with their variety of signatures of energy release including prominences, solar flares, coronal mass ejections (CMEs), radio emissions, fluxes of solar energetic particles (SEPs) and global waves, play a significant role in generating space weather. Large eruptions can evolve into CMEs that can plow through the solar wind and ultimately impact the Earth's magnetosphere [2, 3]. Many of these CMEs were claimed to originate from prominence eruptions [4]. Regardless of their magnitude, eruptions are key elements in figuring out the structure and dynamics of the solar atmosphere [5].

Solar eruptions demonstrate the solar activity − they might be a simple local brightening or the most powerful event in our solar system. The easiest to observe are the bright chromospheric eruptions. Typically, they are visible in H_α and are evidence of some deep-seated disturbance which may manifest itself at widely separated points on the Sun [6]. Observations of solar eruptive events at radio frequencies started a few years after the first detection of radio waves from an astronomical object in 1932 by Karl Jansky and often the radio bursts are associated with chromospheric eruptions [7, 8].

The occurrence of solar eruption often happens after a disparition brusque (DB) of a filament. DBs are events observed in H_α, first reported by Deslandres in 1889 [9]. They are a kind of filament eruptions (FEs) and may be a final or a temporary change in shape and visibility of the prominence [10]. Nearly half of low-latitude filaments are seen to suffer a DB at least once during their existence [11]. Two types of DBs are known − thermal (DBt [12]) and dynamical (DBd [13]). DBds are classical eruptions of a quiescent filament when the prominence plasma is ejected in the corona and in the heliosphere. In most of the cases DBds are final stage of prominence lifetime. The DBts on the other hand happen due to heating of the cold prominence material because of rising energy flux to the body of the filament. It disappears in H_α line, but becomes visible in UV or X-rays. Often the prominence appears again in H_α in a few hours when cooling down. The DBds are more often associated with CMEs of intense geomagnetic storms [14, 15, 4].

CMEs consist of large structures containing plasma and magnetic fields that are expelled from the Sun into the heliosphere with the apparent speeds of the leading edges of CMEs range from about 20 to $>2500\ \mathrm{km\,s^{-1}}$, or from well below the sound speed in the corona to well above the Alfvèn speed [16, 17]. White-light observations reveal the typical structure of a CME: bright loop (helmet streamer) with a dark cavity below and a core [18] − structures that can also appear in the quiet solar atmosphere [19, 20]. The CME core consists a filament [21]. Various studies explore the relation between different manifestations of solar activity. It was found that approximately half of active region (AR) FEs are associated with CMEs [22]. Smaller eruptions may provide the ultimate source for the solar wind [23]. As the FEs are claimed to be progenitors of mass ejections, different authors reveal different values of this relation: 56% by [24], or more than 80% by [25, 4]. CME-related are 92% of studied eruptive prominences by [26], while the remaining 8% "show weak mass motions confined to nearby streamers".

While studying the relationship between different solar phenomena [24] divide FEs in two groups − active and quiescent. For a "solar flare" defined as the enhanced emission either in optical H_α or/and in GOES X-ray, 41% of all prominence eruptions are linked with flares by [24]. AR FEs are more likely to be associated with flares (95%) compared to quiescent FEs (28%). Similar results are obtained using larger samples by [22], connecting 96% of FEs with flares.

No statistical relationship is been reported between FEs and SEP fluxes (above 10 MeV). Previous studies discuss only isolated cases, e.g., single event studies are shown in [27, 28, 29] and a handful of events are analyzed by [30, 31]. Overall, the authors claimed that AR and impulsive phase are not necessary for the occurrence of the SEP events that were characterized by a rather steep spectrum ($\gtrsim$4). CME-driven shock acceleration scenario was favored there, supported by the observation of IP type II radio bursts (without metric type II or shock-signatures formed only in the high corona).

The aim of this study is to re-evaluate the association between filaments and SEP events using larger event samples than before and the best quality prominence observations possible to date. Thus, the analysis covers the time period of Solar Dynamics Observatory (SDO [32]) mission. Namely, a list of observed SEP events from 2010 to the end of 2016 has been systematically checked for the appearance or not of a prominence. The reversed direction of the correspondence has also been evaluated, using all reported SDO FEs [33]. The association rate and characteristics of the filaments are finally compared with the respective properties of all FEs.

2. Observations and Data Analysis

For the analysis performed in this study, several different types of data and catalogs are used. The main components of the work are the prominences and SEP (with a focus on the proton) events.

Space-based observations by the Atmospheric Imaging Assembly (AIA; [34]) aboard the SDO are the main source for the prominence data analysis. We analyzed images from HeII 304 Å channel taken with spatial resolution of $\sim 1.5''$ and a cadence of about 12 seconds. To check for possible association between the filaments and ARs we inspected images in AIA 1600 Å, 1700 Å and 4500 Å and used the provided AR identification by https://solarmonitor.org.

In addition, a list of AIA/SDO FEs has already been compiled by [33] and provided as online catalog[1] with $\gtrsim$900 entries over the period 2010−2014. Among all parameters listed in the catalog, relevant for our study are the onset and end times of the FE together with the related flare and CME. Based on these timings, we could associate the SOHO/ERNE proton event with the given FE.

For the energetic proton events, data from the SOHO/ERNE [35] instrument is used. In the considered period (2010−2016), 186 proton events in the 17−22 MeV energy channel have been identified by visual inspection of the temporal profiles of the proton fluxes. Furthermore, we applied a temporal criteria for the association between the in situ proton event and the solar eruptive event, in terms of both solar flare and CME, where possible, similarly to the procedure summarized in [36]. For 111/186 (60%) of proton events both flare and CME could be identified, whereas for the additional 45 proton cases only one of the eruptive event could be associated (due to data gaps, complex cases or high amount of uncertainty). For the remaining 30 proton cases, no solar origin association could be found and these events are not considered further in this study. Finally, a filament is sought at the time of onset of the solar flare/CME, regarded as the solar origin of the proton event. A detailed report on the SOHO/ERNE 20 MeV catalog compilation is under way (for preliminary results see [37]).

Among the additional information relevant for the present study are the flare listing[2],[3], radio burst identification [36] and the LASCO/SOHO (Large Angle and Spectrometric Coronagraph Experiment/Solar and Heliospheric Observatory) CME Catalog[4] [38]. Sunspot number data used for graphical representation of the solar cycle is taken from SILSO data archive, Royal

[1] http://aia.cfa.harvard.edu/filament/
[2] https://hesperia.gsfc.nasa.gov/goes/goes_event_listings/
[3] ftp://ftp.ngdc.noaa.gov/STP/SOLAR_DATA/SGD_PDFversion/
[4] https://cdaw.gsfc.nasa.gov/CME_list/

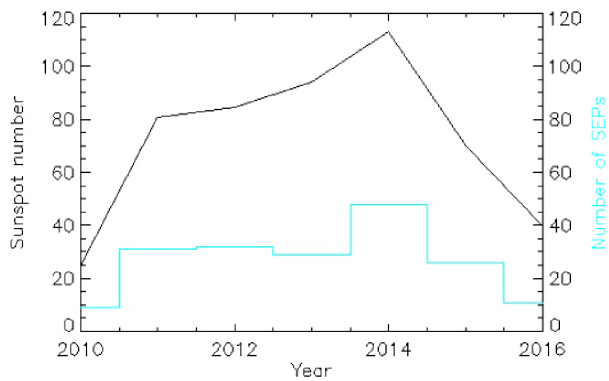

Figure 1: Yearly distribution of the proton events and yearly mean total sunspot number.

Observatory of Belgium, Brussels[5].

The characteristics of the protons, filaments and related phenomena are summarized in a table form in the Appendix.

3. Results

3.1. Correlation analysis between solar proton events and filaments

In the time period considered by the current study (2010−2016), there are 186 proton events at ∼20 MeV identified by SOHO/ERNE instrument. When studying the solar origin of SEP events we exclude all events with uncertain origin identification. Thus only about 84% (156/186) from the original proton list remains to be explored. Using the information for the proton-related flares and CMEs, we identified the presence or not of a filament (no distinction between eruptive or not). From our list, 82/156 SEP events were accompanied by prominences (53%), while in the remaining 74/156 cases (47%) could not be associated with any filaments.

The frequency of SEP occurrence increases around the solar maximum. (Figure 1). The maximum of solar cycle 24 (as defined by sunspot number) reached in April 2014 coincides well with the maximum of registered proton events. The heliographic (longitude and latitude) distribution of the proton events is given in Figure 2. SEP events with identified origin and (flare) heliographic coordinates tend to appear in an area ±30° around the

[5] http://sidc.be/silso/datafiles

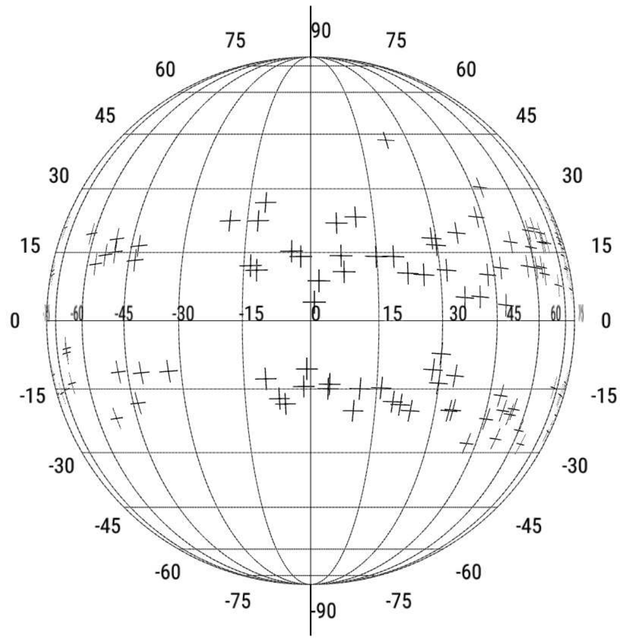

Figure 2: Heliographic locations of the origin of the SEP events registered by SOHO/ERNE in the period 2010 and 2016.

solar equator, preferring latitudes around $\pm 15°$. The expected north-south asymmetry for the explored time period between 2010 and 2016 is noticeable even after excluding 74 events with unknown flare coordinates. We obtain that 59% (66/112 cases) of the particle origin are observed north of the solar equator and 41% (46/112 cases) − to the south. In addition, we mark that SEPs appear mostly in northern hemisphere before the maximum of solar cycle 24 (accepted here to be April 2014) and prefer southern hemisphere after the solar maximum.

When evaluating the heliolongitude of the proton origin, in addition to the information of the AR location taken from the proton-related flare, we also use the direction of propagation of the proton-related CME (given by the measurement position angle, MPA). Since at least one of the flare−CME pair is identified for 156 proton events, AR and MPA information is used. Finally, we obtain that nearly 69% (108/156) of the proton sample originate from the western heliolongitudes, whereas the remaining 31% (48/156) are from the east. These percentages confirm the well-known observation for the preferential western origin of in situ observed particles. This trend is kept

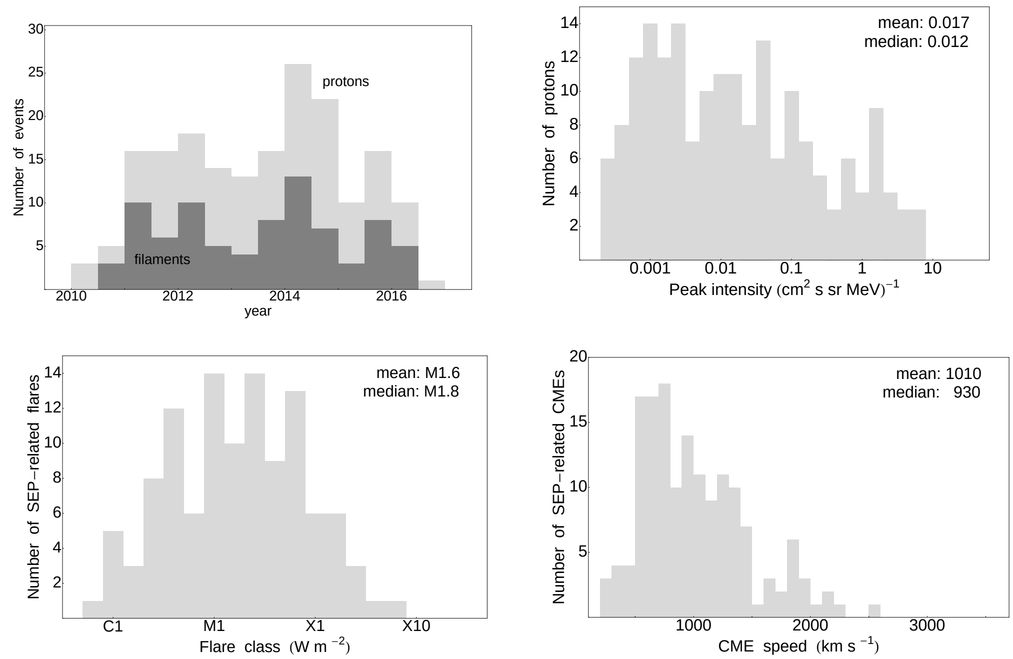

Figure 3: The upper row shows the histograms of the yearly distribution of SOHO/ERNE 20 MeV protons (light-gray) with proton-related filaments (black) on the left and the distribution of the events with respect to the proton peak intensity, right plot. In the lower row, the histograms of the distribution of the number of proton-related solar flares vs. flare class (left) and proton-related CMEs vs. linear speed (right plot) are given.

even when we consider the longitudinal distribution of the proton-related filaments, with 73% (60/82) in the west and 27% (22/82) in the east.

Figure 3 (top left) shows the yearly distribution of the proton and proton-related filaments using 6-month time bin. On the top right plot is presented the distribution of the proton events with respect to the peak intensity (in units of protons/(cm^2 s sr MeV)$^{-1}$). The mean/median values are 0.017/0.012, respectively.

For completeness, we present the distributions of the proton-related flare and CME sample (lower row), as a function of their flare class and CME speed, correspondingly. The mean/median values (M1.6/M1.8 and 1010/930 km s^{-1}) are shown in each respective plot.

The association rate between SEP-related filaments and ARs is 87%. Only 11 (about 13%) of the 82 SEP-related prominences are not connected with AR. Heliographic coordinates could be found for half of these filaments,

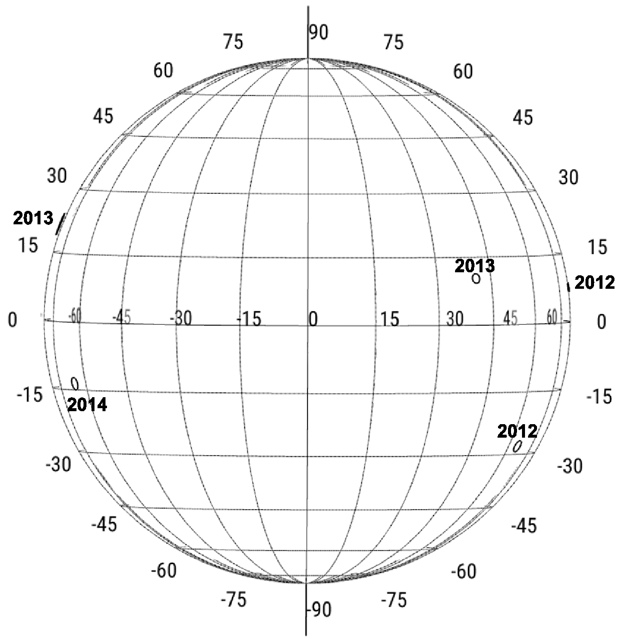

Figure 4: Distribution of the SEP-related prominences outside active regions with known heliographic coordinates.

as marked on Figure 4, whereas for the remaining cases the flare is uncertain and thus the heliographic location.

Furthermore, we identified the type II burst occurrence (used as a proxy for a shock wave) to each reported proton case using as a guideline the timing of the flare and CME. Part of the associations are adopted from the catalog in [39], whereas the remaining cases are identified following the procedure described there. Based on the possible identification, we summarize in Table 1 the occurrence or not of a coronal or IP type II radio burst with respect to the protons with and without filaments. In total, 149 identifications were possible for the coronal range (in 84 of the cases, type II are present) and 152 for the IP range (90 IP type II could be identified). From the entire list of 186 proton events, there are also a number of uncertain cases in either range, namely when no type II burst could be identified with certainty (37 in the coronal and 34 in the IP range). When we normalize to the event sample, we will drop the uncertain cases.

From the 82 proton cases with filaments, 78 have identified radio signatures in the corona and 81 in the IP space, used for the respective nor-

Table 1: Contingency table of the association rate between protons with/without filaments and the type II radio bursts occurring in the solar corona (using ground-based) and IP space (using satellite observations).

Proton-related sample	coronal type II		IP type II	
	Y	N	Y	N
with filaments	62% (48/78)	38% (30/78)	63% (51/81)	37% (30/81)
without filaments	51% (36/71)	49% (35/71)	52% (35/67)	48% (32/67)

malization. The results for the latter show that there is some tendency for proton events with filaments to be accompanied by coronal type II bursts (62%) and/or by IP type IIs (63%) than otherwise, see Table 1. In contrast, when the proton events are not accompanied by filaments (after dropping 3 (7) cases with uncertain coronal (IP) radio signatures, respectively from the total sample of 74 proton events without filaments), the percentages of occurrence or not of type II burst are nearly the same.

As a rule, the above percentage in the coronal range is calculated independently on the findings in the IP one. However, one could impose different set of criteria on the appearance for the coronal and IP type II bursts. Requiring information for the type IIs to be known in both radio ranges, we are left with 145 cases from the entire proton sample. Among them, 77 (68) are for protons with (without) filaments. When implying the condition of simultaneous occurrence of coronal and IP type II burst, we obtain 47% (36/77) for the protons with filaments and 38% (26/68) for the protons without the presence of a filament. Furthermore, if we require a coronal type II that could not propagate through the IP space, the results are nearly equal for either category, 14%, 11/77 (with) and 15%, 10/68 (without). Similar results are obtained when no coronal but a presence only of IP signature is required, 18%, 14/77 (19%, 13/68) for proton events with (without filaments), respectively. The remaining percentages (16 and 19 events) are for the proton cases with lack of type II bursts in both radio ranges, for the presence or not of filaments, respectively.

3.2. Correlation analysis between FEs and solar proton events

The reverse direction of the association is by considering protons related to filaments. However, no comprehensive list of all observed filaments during the period of interest is known to us. Nevertheless, a list of FEs is available and is used in this study, the AIA catalog of FEs [33]. The online version of the catalog[6] contains close to 980 entries in the period April 2010−October 2014, however only about 954 are selected here for further analysis (after removal of double entires). Since this is not a list of all observed filaments (quiescent and eruptive), the reverse association is performed with the additional condition applied on the filaments to be eruptive. In the same period 2010−2014 as the AIA FE catalog, 37 out of the 65 proton-related filaments (see Appendix) are not listed in the FE catalog, probably due to lack of apparent eruption. For the purpose of comparison as well as due to the large number of FEs and its availability, the AIA FE catalog is adopted here as a representative FE list.

The analysis starts with the timings provided for the FEs together with information about the identified accompanied solar features (flares, CMEs, ARs). FEs and the proton events are assumed to be related phenomena if the onset of the proton as measured at 1 AU is either during the course of the FE or latest two hours after the reported end of the FE (in order to allow time for particle acceleration and transport to the particle detector). From the reported FE duration and the onset time of the protons, we could identify only 45 cases that fulfill the above condition, or the probability of occurrence reaches only 5% (45/954). This number should be considered as a lower limit for the association rate, due to the adopted criterion for association and the omissions of filaments from the catalog.

In Figure 5 (upper row) are shown the histograms of the FEs and the FE-related protons. The distribution in terms of proton peak intensity of these FE-relates protons is given on the right plot. The mean/median value for the proton intensity is 0.045/0.022.

For comparative purposes, we give the flare and CME distributions of the respective FE-related samples, Figure 5 (lower row). In this case, the obtained mean/median values are C2.7/C2.3 and 430/390 $\mathrm{km\,s^{-1}}$, respectively. Much lower values (mean and median) for the FE-related flares and CMEs are obtained, compared to the respective values for the proton-related flare and CME samples.

The statistical difference between the proton-related and FE-related samples is investigated using the Kolmogorov-Smirnov test. The results are shown in Table 2. The proton list and FE-proton list is the only pair that could be drawn from the same parent distribution within the 5% confidence

[6] http://aia.cfa.harvard.edu/filament/catalog_table.txt; status February 2018.

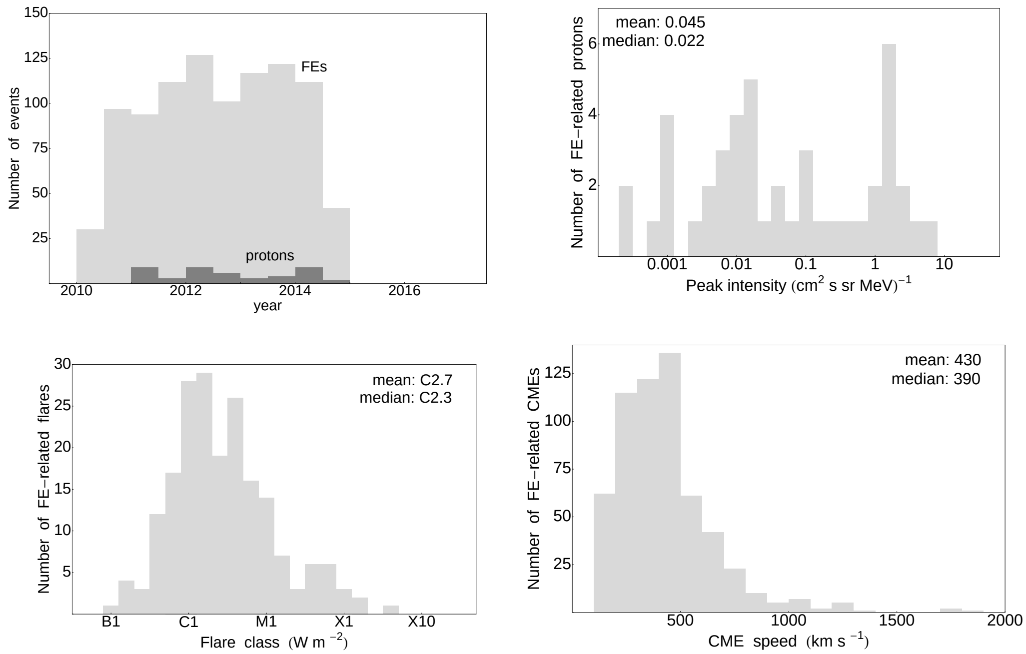

Figure 5: Histogram of the yearly distribution of EPs (light-gray) with FE-related proton events (black) on the left and the distribution of the FE-related proton events with respect to their proton peak intensity, right plot. Histogram of the distribution of the number of FE-related solar flares vs. flare class (left) and FE-related CMEs vs. linear speed (right plot).

Table 2: Table of statistical difference under the Kolmogorov-Smirnov test. A statistical difference between two samples of events is considered when the calculated probability (D) is larger than the reference value for the selected here 5% confidence level, $D_{0.05} = 1.36[(n_1{+}n_2)/n_1{*}n_2]^0.5$, where n_1 and n_2 are the number of events in the two distributions.

	Proton-related and FE-related samples		
	protons	flares	CMEs
difference	No	Yes	Yes
probability	$D = 0.19$; $D_{0.05} = 0.23$	$D = 0.49$; $D_{0.05} = 0.16$	$D = 0.68$; $D_{0.05} = 0.12$
sample size	$n_1 = 186$; $n_2 = 45$	$n_1 = 112$; $n_2 = 197$	$n_1 = 155$; $n_2 = 595$

level, adopted here. Only in case this level is relaxed to about 13%, the two proton distributions show a difference. For the pairs of proton-related and FE-related flare and CME distributions, however, we readily obtain statistical difference. Namely, the proton-related flares and those in association to

FEs comprise two different distributions. Similar result is obtained for the two CME samples. Both, the proton-related flares and CMEs are of larger magnitude, compared to the respective FE-related samples.

4. Conclusions and discussions

We present the most detailed statistical study to date about the connection between solar energetic protons and filaments relying on space-based observations by Atmospheric Imaging Assembly aboard the Solar Dynamics Observatory. We inspected 186 proton events in the period between 2010 and the end of 2016 to identify the related solar activity phenomena (including prominences, flares, coronal mass ejections, radio bursts of type II, etc.). The main results are summarized below:

- Filament-related proton events tend to be slightly more common than non-related (53-to-47 %).
- More SEP events appeared in northern solar hemisphere than in southern for the studied time period (59-to-41 %). The preferred solar hemisphere changes at the year of maximum of solar cycle 24 − in the years before April 2014 more SEP events are observed north of solar equator, while the dependency changes in the second half of the period.
- SEP events appear in a region not farther than $\pm 30°$ around the solar equator. The largest amount of events are detected to originate on about $\pm 15°$ latitude.
- The majority of the SEPs in the considered period is registered to originate from the western hemisphere (close to 70 %).
- 87% of SEP-related filaments are localized in active regions. The remaining 13% consists of only 11 cases for 6 years. The reported cases of prominences outside active regions producing SEP event are rare, such as the events presented by [30, 31]. Two of the reported there events are also listed in the current study (2011/11/26 and 2013/09/29). The one from 2011 is categorized as SEP-related filament out of active region by [31], however we link the filament eruption with AR11353.
- We found that only 5% of the cataloged eruptive filaments tend to produce SEP events.

- Proton events with filaments show a tendency to be accompanied by coronal (62%) and/or IP type II bursts (63%). Among the protons with filaments, 47% have type II features in both ranges, 14% have shock signatures only in the coronal range, 18% − only in the IP range, and the remaining 21% is for the lack of any type II bursts.

Further analysis in several aspects is already under way. The proton catalog (SOHO/ERNE 17−22 MeV) over the previous solar cycle 23 is under completion, allowing the current analysis to be also extended. In addition, the kinematics of the filaments, where permissible to be evaluated by the available observations, will be explored in details. Finally, the filament evolution together with the spectral index characteristics of the filament-related proton events will be the topic of a separate study reported elsewhere.

Acknowledgement

This work was supported by National Science Fund of Bulgaria [contract No. DNTS/Russia 01/6 (23-Jun-2017)].

Appendix

Table 3 lists the SOHO/ERNE 20 MeV proton events and selected parameters of the proton-associated flares, CMEs, filaments and type II radio bursts, using ground-based observations for the coronal signatures and space-borne for the IP features. When a filament has been identified in relation to the proton event, we list the active region (AR) intersected by this filament and whether it is listed in the catalog of filament eruptions [33]. In case of inability to define some characteristic or possible association for the events we use designation ‘u’ for uncertainty, while ‘g’ stands for gap in the data archive of current instrument.

Table 3: Table of ∼20 MeV SOHO/ERNE proton events (2010−2016) and associated solar events: flares (class/onset), CMEs (time of first appearance/linear speed), filaments (Y/N and related AR), appearance of type II radio burst (in the corona: y/n, in the IP space: Y/N), whether the filament is listed in [33] (Y/N). Time in UT; speed in km s^{-1}. Abbreviations: g: data gap; n/N: no; u: uncertain; y/Y: yes.

Proton onset		Solar flare	CME	Filaments		Type	Listed
yyyy/mm/dd	hr	class/onset	time/speed	Y/N	AR	II	Y/N
2010/02/12	17	M8.3/11:19	u	N	-	yN	-
2010/06/12	3	M2.0/00:30	01:32/486	N	-	yY	-
2010/08/14	11	C4.4/09:38	10:12/1205	Y	11097	yY	N
2010/08/18	7	C4.5/04:45	05:48/1471	Y	11098	yY	N
2010/08/31	23	u	21:17/1304	N	-	nY	-
2010/09/08	25	C3.3/23:05	23:27/818	Y	11105	nY	N
2010/12/31	6	C1.3/04:18	05:00/363	N	-	yN	-
2011/01/28	2	M1.3/00:44	01:26/606	Y	11149	yY	Y
2011/02/15	4	X2.2/01:44	02:24/669	Y	11158	yY	Y
2011/03/07	17	C5.8/14:46	15:50/698	Y	11163	yY	N
2011/03/07	22	M3.7/19:43	20:00/2125	Y	11164	yY	Y
2011/03/16	22	C3.7/17:52	19:12/682	Y	11166/11169	uN	N
2011/03/21	5	u	02:24/1341	N	-	yY	-
2011/03/29	22	u	20:36/1264	Y	11180/11183	nN	Y
2011/05/11	4	B8.1/02:23	02:48/745	Y	11203/11205	yY	Y
2011/06/04	12	u	06:48/1407	Y	Y	nY	N
2011/06/07	9	M2.5/06:16	06:49/1255	Y	11233	yY	Y
2011/06/11	13	u	12:00/522	Y	N	nN	Y
2011/08/02	7	M1.4/05:19	06:36/712	N	-	yY	-
2011/08/03	15	M6.0/13:17	14:00/610	N	-	yY	-
2011/08/04	6	M9.3/03:41	04:12/1315	Y	11261	yY	Y
2011/08/08	19	M3.5/18:00	18:12/1343	N	-	yY	-
2011/08/09	9	X6.9/07:48	08:12/1610	N	-	yY	-
2011/09/04	6	C9.0/04:36	05:12/262	N	-	yN	-
2011/09/04	32	C7.9/23:58	00:48/622	N	-	nN	-
2011/09/06	3	M5.3/01:35	02:24/782	Y	11283	yY	Y
2011/09/07	2	X2.1/22:12	23:05/575	Y	11283	yY	Y
2011/09/21	24	u	22:12/1007	N	-	nN	-
2011/10/22	12	M1.3/10:00	10:24/1005	Y	11314	nY	N
2011/11/03	24	M2.1/23:28	23:30/991	Y	11330/11333	nY	N
2011/11/17	8	u	20:36/1041	N	-	nY	-
2011/11/26	9	C1.2/06:09	07:12/933	Y	11353	nY	Y
2012/01/19	19	M3.2/13:44	14:36/1120	Y	11402	nY	Y
2012/01/27	20	C2.4/14:31	15:13/2508	Y	N	yY	-
2012/02/24	5	u	03:46/800	Y	N	nY	-
2012/03/04	19	M2.0/10:29	11:00/1306	Y	11429	nY	N

Table 3: cont'd

Proton onset		Solar flare	CME		EP	Type	Listed
yyyy/mm/dd	hr	class/onset	time/speed	Y/N	AR	II	Y/N
2012/03/07	7	X1.3/01:05	01:30/1825	N	-	yY	-
2012/03/13	19	M7.9/17:12	17:36/1884	Y	11429	nY	N
2012/03/29	31	B6.2/23:19	23:36/753	N	-	nN	-
2012/04/05	24	C1.5/20:49	21:25/828	Y	11450	yY	Y
2012/04/09	15	C3.9/12:12	12:36/921	Y	11452	yY	Y
2012/04/18	42	C1.8/14:42	15:12/540	N	-	nN	-
2012/04/20	3	B9.0/01:55	02:00/345	Y	11463	nN	N
2012/05/17	3	M5.1/01:25	01:48/1582	Y	11476	yY	Y
2012/05/26	22	u	20:58/1966	N	-	yY	-
2012/06/02	7	C1.5/04:15	04:36/1175	N	-	nN	-
2012/06/08	7	C7.7/02:51	03:47/353	N	-	yN	-
2012/06/12	11	u	05:24/864	Y	11494/11499	nN	N
2012/06/14	17	M1.9/12:52	14:12/987	N	-	nY	-
2012/07/06	24	X1.1/23:01	23:24/1828	N	-	yY	-
2012/07/12	18	X1.4/15:37	16:48/885	N	-	yY	-
2012/07/17	16	M1.7/12:03	13:48/958	Y	N	nY	N
2012/07/19	9	M7.7/04:17	05:24/1631	Y	11520	yY	N
2012/07/23	8	u	02:36/2003	Y	11523	yY	Y
2012/08/31	23	C8.4/19:45	20:00/1442	Y	Y	nY	Y
2012/09/08	12	g	10:00/734	N	-	nY	-
2012/09/21	12	u	06:24/639	N	-	nN	-
2012/09/27	g	C3.7/23:36	24:12/947	Y	11575/11577	yY	Y
2012/10/07	16	u	07:36/663	N	-	nN	-
2012/11/08	g	u	11:00/972	N	-	nY	-
2013/02/06	16	C8.7/00:04	00:24/1867	Y	11667	yN	Y
2013/02/26	13	u	09:12/987	N	-	nY	-
2013/03/05	14	u	03:48/1316	N	-	nY	-
2013/03/15	18	M1.1/05:46	07:12/1063	N	-	nY	-
2013/04/11	8	u	07:24/861	N	-	yY	-
2013/04/21	11	u	07:24/919	N	-	nu	-
2013/04/24	24	C1.2/21:50	22:12/594	Y	11723	nN	N
2013/05/02	9	M1.1/04:58	05:24/671	N	-	yN	-
2013/05/13	20	X2.8/15:48	16:08/1850	Y	11745	yY	N
2013/05/15	10	X1.2/01:25	01:48/1366	N	-	yY	-
2013/05/22	15	M5.0/13:08	12:26/1466	Y	11745	yY	N
2013/06/21	13	M2.9/02:30	03:12/1900	Y	11777	nY	N
2013/06/28	8	C4.4/01:36	02:00/1037	N	-	nY	-
2013/08/17	21	M3.3/18:16	19:12/1202	Y	11818	yY	Y
2013/08/20	5	u	08:12/784	N	-	nN	-
2013/08/30	7	C8.3/02:04	02:48/949	N	-	yY	-

Table 3: cont'd

Proton onset		Solar flare	CME	EP		Type	Listed
yyyy/mm/dd	hr	class/onset	time/speed	Y/N	AR	II	Y/N
2013/09/24	32	u	20:36/919	Y	N	nN	Y
2013/09/29	43	C1.2/21:43	22:12/1179	Y	N	yY	Y
2013/10/11	19	M1.5/07:01	07:24/1200	Y	N	yY	N
2013/10/22	24	M4.2/21:15	21:48/459	Y	11873/11875	yY	N
2013/10/25	13	X2.1/14:51	15:12/587	N	-	yY	-
2013/10/28	7	M5.1/04:32	04:48/1201	Y	11875	yY	Y
2013/12/07	12	M1.2/07:17	07:36/1085	Y	Y	yY	N
2013/12/12	6	C4.6/03:11	03:36/1002	N	-	yY	-
2013/12/13	29	u	21:24/518	N	-	nN	-
2013/12/26	8	u	03:34/1336	N	-	nY	-
2013/12/28	20	C9.3/17:53	17:36/1118	N	-	nY	-
2014/01/04	23	M4.0/18:47	21:23/977	N	-	nN	-
2014/01/06	9	u	08:00/1402	Y	11937/11938	yY	Y
2014/01/07	21	X1.2/18:04	18:24/1830	N	-	yY	-
2014/01/20	31	C3.6/21:39	22:00/721	Y	Y	nY	N
2014/01/21	20	M1.3/18:57	18:48/1035	N	-	uN	-
2014/02/11	15	C8.4/13:15	13:48/330	N	-	yN	-
2014/02/11	24	u	19:24/613	Y	11975	uY	N
2014/02/14	13	u	08:48/1165	N	-	nN	-
2014/02/16	11	M1.1/09:20	10:00/634	N	-	nu	-
2014/02/18	5	C3.3/09:49	01:36/779	Y	N	yN	Y
2014/02/20	8	M3.0/07:26	08:00/948	Y	Y	yY	N
2014/02/25	5	X4.9/00:39	01:26/2147	Y	11990	yY	Y
2014/03/22	13	u	10:00/756	N	-	nN	-
2014/03/24	12	u	07:12/809	Y	Y	nN	N
2014/03/28	25	M2.6/23:44	23:48/514	Y	12017	yY	N
2014/03/29	19	X1.0/17:35	18:12/528	N	-	yY	-
2014/04/02	25	M6.5/13:18	13:36/1471	N	-	yY	-
2014/04/05	4	u	06:24/798	N	-	nN	-
2014/04/18	14	M7.3/12:31	13:26/1203	N	-	yY	-
2014/04/25	2	X1.3/00:17	00:48/456	Y	12046	yN	N
2014/05/07	19	M1.2/16:07	16:24/923	Y	12055/12056	nY	N
2014/05/09	4	u	02:48/1099	Y	12049	yY	Y
2014/06/06	13	u	12:48/704	Y	N	yN	N
2014/06/12	25	M3.1/21:34	22:12/684	Y	12085	yY	N
2014/06/17	17	C3.0/08:13	09:12/1198	N	-	nN	-
2014/07/08	18	M6.5/16:06	16:36/773	Y	12113	yN	Y
2014/08/22	13	u	11:12/600	N	-	yY	-
2014/08/25	18	M2.0/14:46	15:36/55	N	-	yY	-
2014/08/29	3	u	17:24/766	N	-	uN	-

Table 3: cont'd

Proton onset		Solar flare	CME		EP	Type	Listed
yyyy/mm/dd	hr	class/onset	time/speed	Y/N	AR	II	Y/N
2014/09/02	5	u	11:12/1901	N	-	yY	-
2014/09/10	26	X1.6/17:21	18:00/1267	N	-	yY	-
2014/09/22	9	u	06:12/618	N	-	nY	-
2014/09/24	30	u	21:30/1350	N	-	yY	-
2014/10/02	21	M7.3/18:49	19:12/513	Y	12173	yN	N
2014/10/10	19	C3.0/15:42	16:12/782	N	-	nN	-
2014/10/13	4	u	00:12/521	Y	12184	nN	N
2014/10/15	24	M2.2/19:07	18:48/848	Y	12129	uN	N
2014/11/01	9	C2.7/04:44	05:00/1628	Y	12200	yu	-
2014/11/07	6	M2.0/04:12	04:38/672	N	-	nu	-
2014/11/09	14	u	10:24/633	Y	12207	nN	-
2014/11/10	11	C7.6/02:18	03:36/230	N	-	nN	-
2014/12/05	8	C2.1/05:28	06:24/534	N	-	yN	-
2014/12/13	11	g	14:24/2222	Y	12227	yY	-
2015/02/21	11	u	09:24/1120	Y	N	nN	-
2015/04/12	26	C6.4/23:24	23:48/678	Y	12320	yN	-
2015/04/14	15	u	02:36/1198	N	-	yN	-
2015/05/06	15	M1.9/11:45	12:12/738	N	-	yN	-
2015/05/12	5	C2.6/02:15	02:48/772	Y	12335/12337	yN	-
2015/06/14	8	C5.9/03:48	04:12/1228	N	-	nN	-
2015/06/18	4	M1.2/00:33	01:26/1714	Y	12365	nN	-
2015/06/21	19	M2.6/02:06	02:36/1366	N	-	yY	-
2015/07/01	16	u	14:36/1435	Y	N	uY	-
2015/07/19	12	C2.1/09:22	09:48/782	Y	12384	nN	-
2015/08/24	10	M5.6/07:26	08:48/272	Y	12403	nN	-
2015/09/20	19	M2.1/17:32	18:12/1239	Y	12418	yY	-
2015/09/30	19	g	09:36/586	Y	12422	nN	-
2015/10/22	7	C4.4/02:13	03:12/817	N	-	nN	-
2015/10/29	3	u	02:36/530	Y	12437	yY	-
2015/11/04	16	M3.7/13:31	14:48/578	N	-	yY	-
2015/11/09	22	M3.9/12:49	13:25/1041	Y	12449	yY	-
2015/12/28	14	M1.8/11:20	12:12/1212	N	-	nY	-
2016/01/01	24	M2.3/23:10	23:24/1730	Y	12473	yN	-
2016/01/28	13	C9.6/11:48	12:24/562	Y	12488	nN	-
2016/01/29	24	C2.0/20:48	22:12/800	Y	12488	nN	-
2016/02/11	27	C8.9/20:18	21:18/719	N	-	yN	-
2016/03/16	8	C2.2/06:34	07:00/592	Y	12522	yN	-
2016/04/18	27	M6.7/00:14	00:48/1084	Y	Y	yN	-
2016/05/15	17	C3.2/15:19	15:12/1118	N	-	uN	-
2016/07/20	25	C4.6/22:03	23:12/426	N	-	nN	-

References

[1] E. Priest, Magnetohydrodynamics of the Sun, 2014.

[2] R. H. Munro, J. T. Gosling, E. Hildner, R. M. MacQueen, A. I. Poland, C. L. Ross, The association of coronal mass ejection transients with other forms of solar activity, *Solar Phys.*61 (1979) 201–215. doi:10.1007/BF00155456.

[3] J. T. Gosling, The solar flare myth, *J. Geophys. Res.*98 (1993) 18937–18950. doi:10.1029/93JA01896.

[4] N. Gopalswamy, M. Shimojo, W. Lu, S. Yashiro, K. Shibasaki, R. A. Howard, Prominence Eruptions and Coronal Mass Ejection: A Statistical Study Using Microwave Observations, *Astrophys. J.*586 (2003) 562–578. doi:10.1086/367614.

[5] N. Hurlburt, Automated detection of solar eruptions, Journal of Space Weather and Space Climate 5 (27) (2015) A39. arXiv:1504.03395, doi:10.1051/swsc/2015042.

[6] R. S. Richardson, The Nature of Bright Chromospheric Eruptions, *Pub. Astron. Soc. Pac.*49 (1937) 233–239. doi:10.1086/124834.

[7] H. W. Newton, H. J. Barton, Bright solar eruptions and radio fadings during the years 1935-36, *Mon. Not. Roy. Astron. Soc.*97 (1937) 594. doi:10.1093/mnras/97.8.594.

[8] R. S. Richardson, Relation between Bright Chromospheric Eruptions and Fade-Outs of High-Frequency Radio Transmission, *Pub. Astron. Soc. Pac.*49 (1937) 82. doi:10.1086/124772.

[9] E. Tandberg-Hanssen (Ed.), The nature of solar prominences, Vol. 199 of Astrophysics and Space Science Library, 1995. doi:10.1007/978-94-017-3396-0.

[10] M. A. Raadu, J. M. Malherbe, B. Schmieder, P. Mein, Material ejecta in a disturbed solar filament, *Solar Phys.*109 (1987) 59–79. doi:10.1007/BF00167399.

[11] L. D'Azambuja, Ph.D. thesis, Thesis at the Observatory of Paris, (1948) (1948).

[12] Z. Mouradian, M. J. Martres, I. Soru-Escaut, The heating of filaments as a disappearance process, in: A. I. Poland (Ed.), NASA Conference Publication, Vol. 2442 of NASA Conference Publication, 1986.

[13] P. Demoulin, J. C. Vial, Structural characteristics of eruptive prominences, *Solar Phys.*141 (1992) 289–301. doi:10.1007/BF00155181.

[14] L. Taliashvili, Z. Mouradian, J. Páez, Dynamic and Thermal Disappearance of Prominences and Their Geoeffectiveness, *Solar Phys.*258 (2009) 277–295. doi:10.1007/s11207-009-9414-x.

[15] B. Schmieder, C. Delannée, D. Y. Yong, J. C. Vial, M. Madjarska, Multi-wavelength study of the slow "disparition brusque" of a filament observed with SOHO, *Astron. Astrophys.*358 (2000) 728–740.

[16] D. F. Webb, T. A. Howard, Coronal Mass Ejections: Observations, Living Reviews in Solar Physics 9 (2012) 3. doi:10.12942/lrsp-2012-3.

[17] P. F. Chen, Coronal Mass Ejections: Models and Their Observational Basis, Living Reviews in Solar Physics 8 (2011) 1. doi:10.12942/lrsp-2011-1.

[18] R. M. E. Illing, A. J. Hundhausen, Disruption of a coronal streamer by an eruptive prominence and coronal mass ejection, *J. Geophys. Res.*91 (1986) 10951–10960. doi:10.1029/JA091iA10p10951.

[19] K. Saito, E. Tandberg-Hanssen, The Arch Systems, Cavities, and Prominences in the Helmet Streamer Observed at the Solar Eclipse, November 12, 1966, *Solar Phys.*31 (1973) 105–121. doi:10.1007/BF00156076.

[20] S. E. Gibson, D. Foster, J. Burkepile, G. de Toma, A. Stanger, The Calm before the Storm: The Link between Quiescent Cavities and Coronal Mass Ejections, *Astrophys. J.*641 (2006) 590–605. doi:10.1086/500446.

[21] L. L. House, W. J. Wagner, E. Hildner, C. Sawyer, H. U. Schmidt, Studies of the corona with the Solar Maximum Mission coronagraph/polarimeter, *Astrophys. J. Lett.*244 (1981) L117–L121. doi:10.1086/183494.

[22] X.-L. Yan, Z.-Q. Qu, D.-F. Kong, Relationship between eruptions of active-region filaments and associated flares and coronal mass ejections, *Mon. Not. Roy. Astron. Soc.*414 (2011) 2803–2811. arXiv:1101.3625, doi:10.1111/j.1365-2966.2011.18336.x.

[23] H. Tian, E. E. DeLuca, S. R. Cranmer, B. De Pontieu, H. Peter, J. Martínez-Sykora, L. Golub, S. McKillop, K. K. Reeves, M. P. Miralles, P. McCauley, S. Saar, P. Testa, M. Weber, N. Murphy, J. Lemen, A. Title, P. Boerner, N. Hurlburt, T. D. Tarbell, J. P. Wuelser, L. Kleint, C. Kankelborg, S. Jaeggli, M. Carlsson, V. Hansteen, S. W. McIntosh, Prevalence of small-scale jets from the networks of the solar transition region and chromosphere, Science 346 (27) (2014) 1255711. arXiv:1410.6143, doi:10.1126/science.1255711.

[24] J. Jing, V. B. Yurchyshyn, G. Yang, Y. Xu, H. Wang, On the Relation between Filament Eruptions, Flares, and Coronal Mass Ejections, *Astrophys. J.*614 (2004) 1054–1062. doi:10.1086/423781.

[25] B. Schmieder, P. Demoulin, G. Aulanier, Title, in: 39th COSPAR Scientific Assembly, Vol. 39 of COSPAR Meeting, 2012, p. 1.

[26] K. Hori, J. L. Culhane, Trajectories of microwave prominence eruptions, *Astron. Astrophys.*382 (2002) 666–677. doi:10.1051/0004-6361:20011658.

[27] C. L. Hyder, A Phenomenological Model for Disparitions Brusques followed by Flarelike Chromospheric Brightenings, I: The Model, its Consequences, and Observations in Quiet Solar Regions, *Solar Phys.*2 (1967) 49–74. doi:10.1007/BF00155892.

[28] S. W. Kahler, E. W. Cliver, H. V. Cane, R. E. McGuire, R. G. Stone, N. R. Sheeley, Jr., Solar filament eruptions and energetic particle events, *Astrophys. J.*302 (1986) 504–510. doi:10.1086/164009.

[29] S. W. Kahler, Origin and properties of solar energetic particles in space, Washington DC American Geophysical Union Geophysical Monograph Series 125 (2001) 109–122. doi:10.1029/GM125p0109.

[30] S. Kahler, N. Gopalswamy, P. Makela, S. Akiyama, S. Yashiro, H. Xie, N. Thakur, Filament Eruptions Outside of Active Regions as Sources

of Large Solar Energetic Particle Events, in: 34th International Cosmic Ray Conference (ICRC2015), Vol. 34 of International Cosmic Ray Conference, 2015, p. 48.

[31] N. Gopalswamy, P. Mäkelä, S. Akiyama, S. Yashiro, H. Xie, N. Thakur, S. W. Kahler, Large Solar Energetic Particle Events Associated with Filament Eruptions Outside of Active Regions, *Astrophys. J.*806 (2015) 8. arXiv:1504.00709, doi:10.1088/0004-637X/806/1/8.

[32] W. D. Pesnell, B. J. Thompson, P. C. Chamberlin, The Solar Dynamics Observatory (SDO), *Solar Phys.*275 (2012) 3–15. doi:10.1007/s11207-011-9841-3.

[33] P. I. McCauley, Y. N. Su, N. Schanche, K. E. Evans, C. Su, S. McKillop, K. K. Reeves, Prominence and Filament Eruptions Observed by the Solar Dynamics Observatory: Statistical Properties, Kinematics, and Online Catalog, *Solar Phys.*290 (2015) 1703–1740. arXiv:1505.02090, doi:10.1007/s11207-015-0699-7.

[34] J. R. Lemen, A. M. Title, D. J. Akin, P. F. Boerner, C. Chou, J. F. Drake, D. W. Duncan, C. G. Edwards, F. M. Friedlaender, G. F. Heyman, N. E. Hurlburt, N. L. Katz, G. D. Kushner, M. Levay, R. W. Lindgren, D. P. Mathur, E. L. McFeaters, S. Mitchell, R. A. Rehse, C. J. Schrijver, L. A. Springer, R. A. Stern, T. D. Tarbell, J.-P. Wuelser, C. J. Wolfson, C. Yanari, J. A. Bookbinder, P. N. Cheimets, D. Caldwell, E. E. Deluca, R. Gates, L. Golub, S. Park, W. A. Podgorski, R. I. Bush, P. H. Scherrer, M. A. Gummin, P. Smith, G. Auker, P. Jerram, P. Pool, R. Soufli, D. L. Windt, S. Beardsley, M. Clapp, J. Lang, N. Waltham, The Atmospheric Imaging Assembly (AIA) on the Solar Dynamics Observatory (SDO), *Solar Phys.*275 (2012) 17–40. doi:10.1007/s11207-011-9776-8.

[35] J. Torsti, E. Valtonen, M. Lumme, P. Peltonen, T. Eronen, M. Louhola, E. Riihonen, G. Schultz, M. Teittinen, K. Ahola, C. Holmlund, V. Kelhä, K. Leppälä, P. Ruuska, E. Strömmer, Energetic Particle Experiment ERNE, Solar Physics 162 (1995) 505–531. doi:10.1007/BF00733438.

[36] R. Miteva, S. W. Samwel, M. V. Costa-Duarte, The Wind/EPACT Proton Event Catalog (1996 - 2016), *Solar Phys.*293 (2018) id. 27. arXiv:1801.00469, doi:10.1007/s11207-018-1241-5.

[37] R. Miteva, SOHO/ERNE proton event catalog: Description and first results, in: G. Mardirossian, T. Srebrova, G. Jelev (Eds.), Space, Ecology, Safety - SES 2017, Thirteenth International Scientific conference "Space, Ecology, Safety - SES1027", held 2-4 November 2017 in Sofia, Bulgaria. Edited by G. Mardirossian, Ts. Srebrova and G. Jelev. ISSN: 1313-3888, p. 52-56, 2017, pp. 52–56.

[38] N. Gopalswamy, S. Yashiro, G. Michalek, G. Stenborg, A. Vourlidas, S. Freeland, R. Howard, The SOHO/LASCO CME Catalog, Earth Moon and Planets 104 (2009) 295–313. doi:10.1007/s11038-008-9282-7.

[39] R. Miteva, S. W. Samwel, V. Krupar, Solar energetic particles and radio burst emission, Journal of Space Weather and Space Climate 7 (27) (2017) A37. arXiv:1711.09348, doi:10.1051/swsc/2017035.

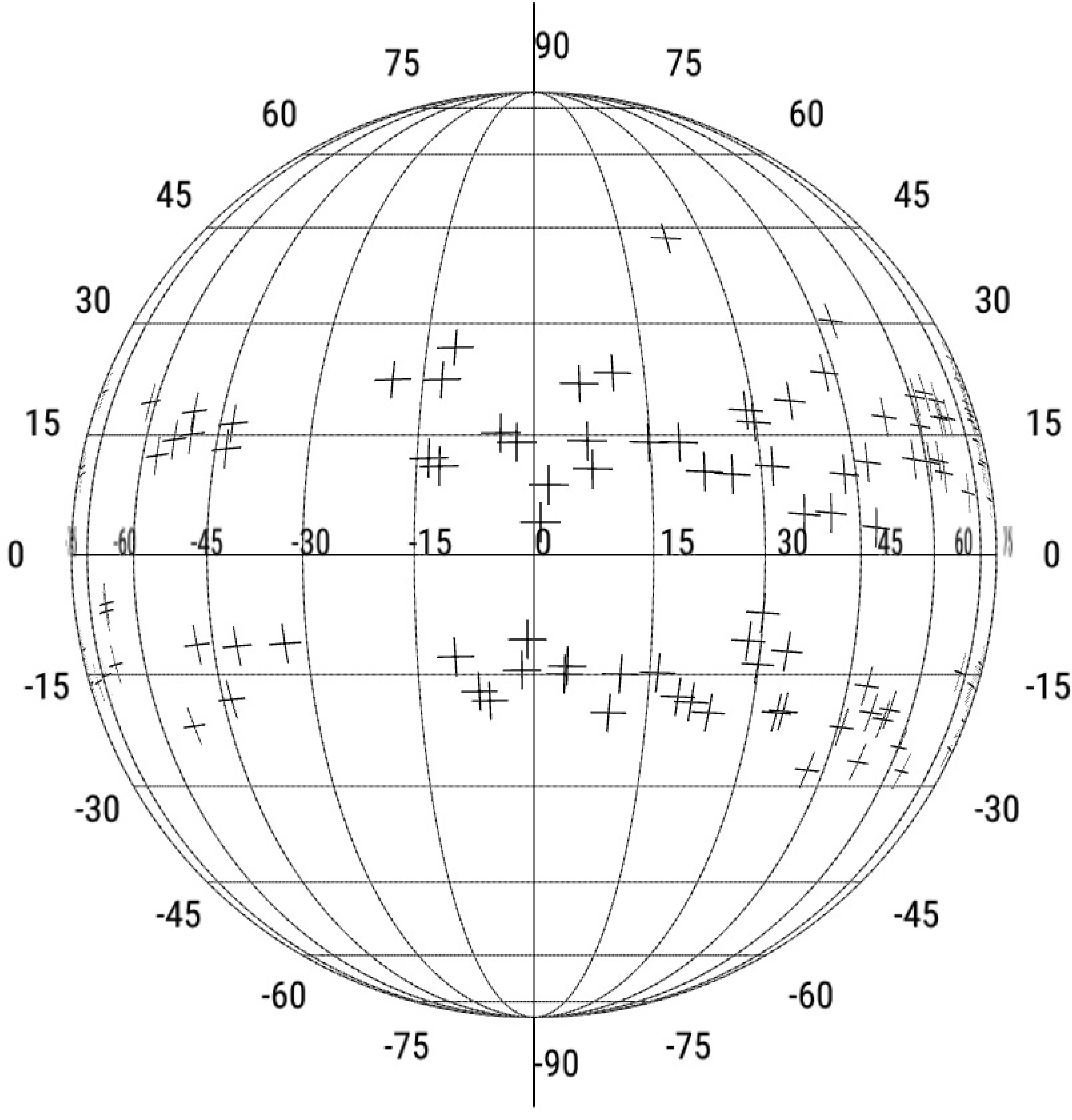
90
75
75
60
60
45
45
30
30
15
15
0
-60
-45
-30
-15
0
15
30
45
60
0
-15
-15
-30
-30
-45
-45
-60
-60
-75
-75
-90

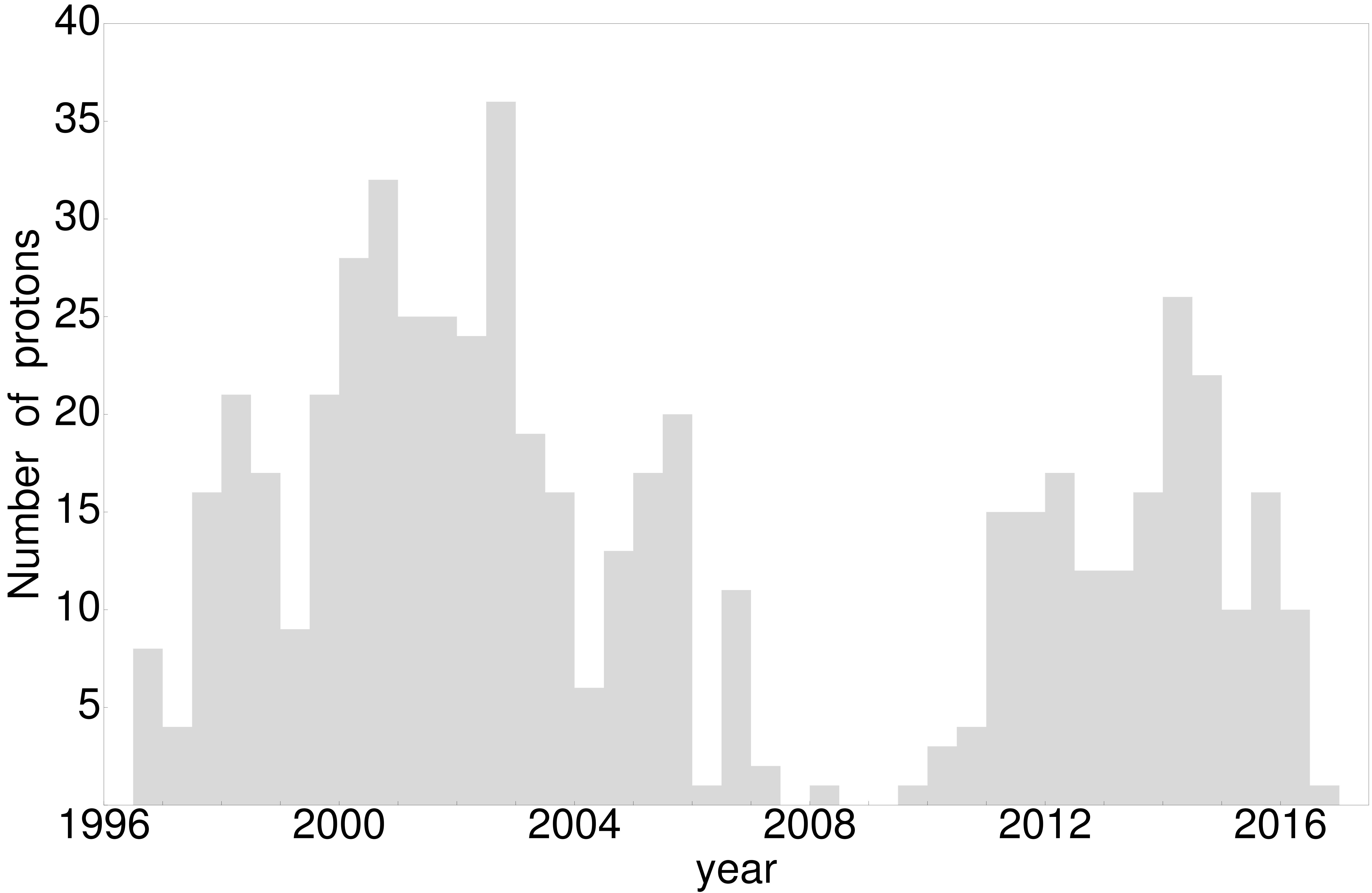

40
35
30
25
20
15
10
5
Number of protons
1996
2000
2004
2008
2012
2016
year

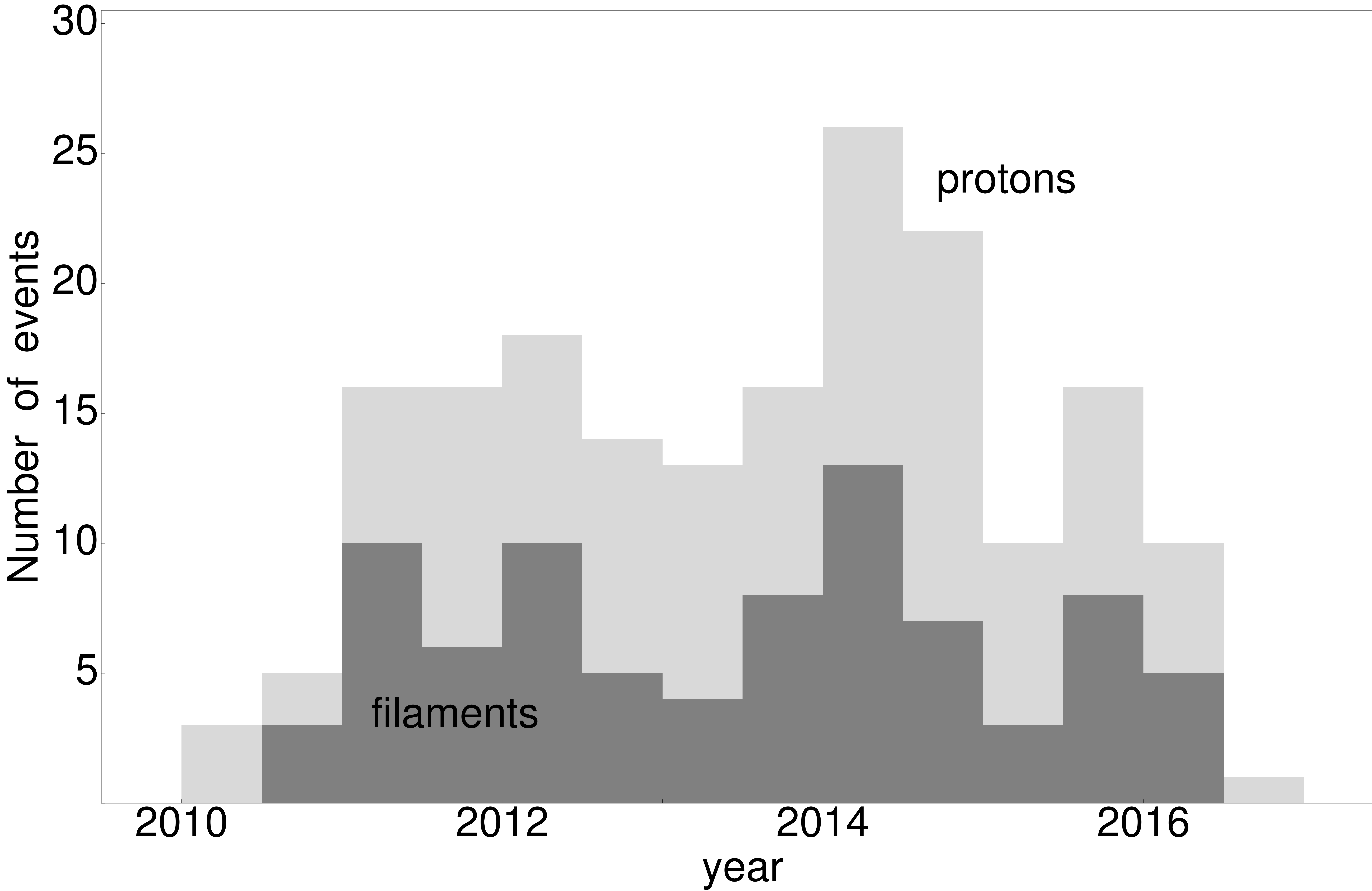

30
25
20
15
10
5
Number of events
protons
filaments
2010
2012
2014
2016
year

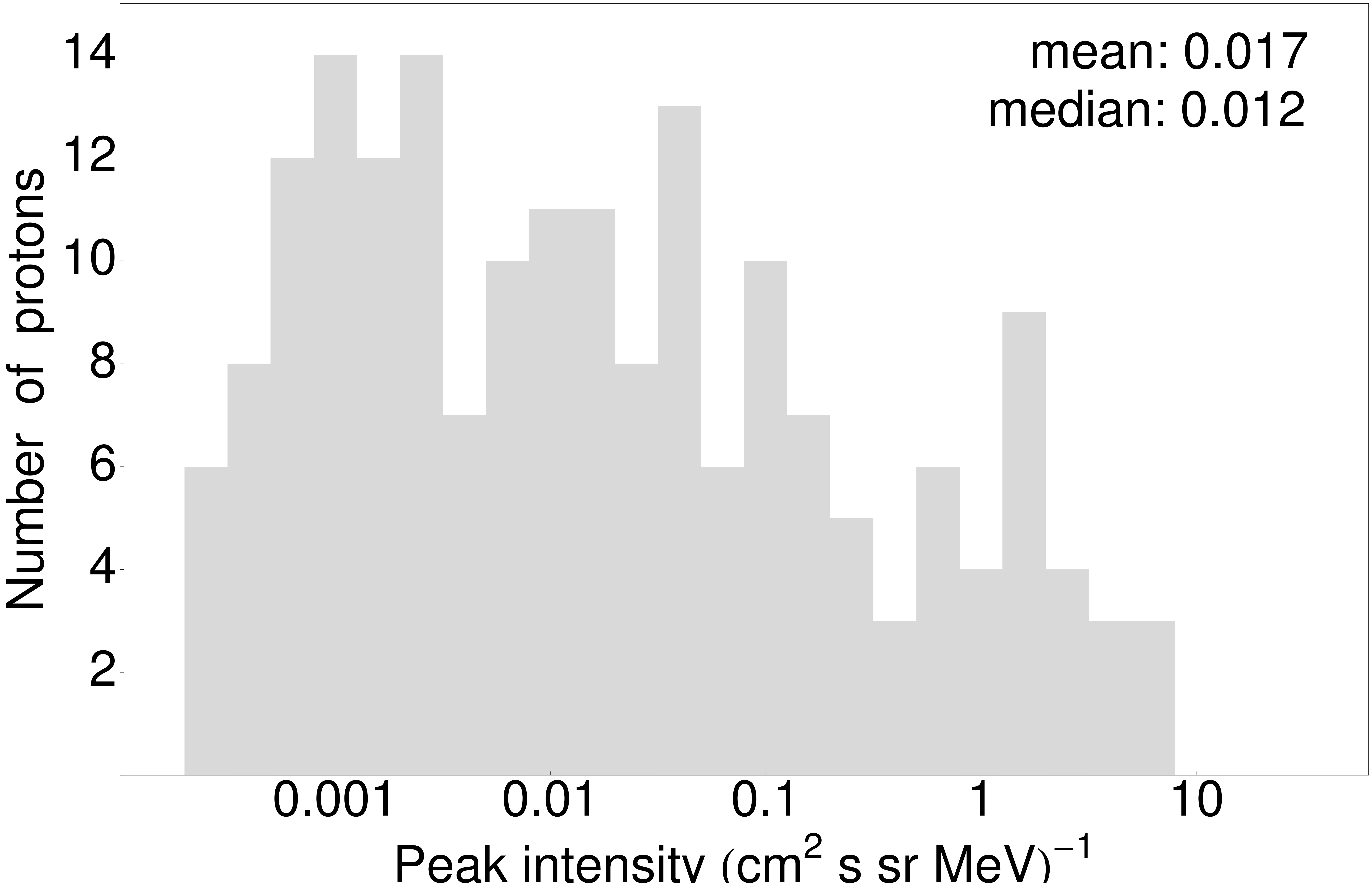

mean: 0.017
median: 0.012
Number of protons
14
12
10
8
6
4
2
0.001
0.01
0.1
1
10
Peak intensity (cm^2 s sr MeV)$^{-1}$

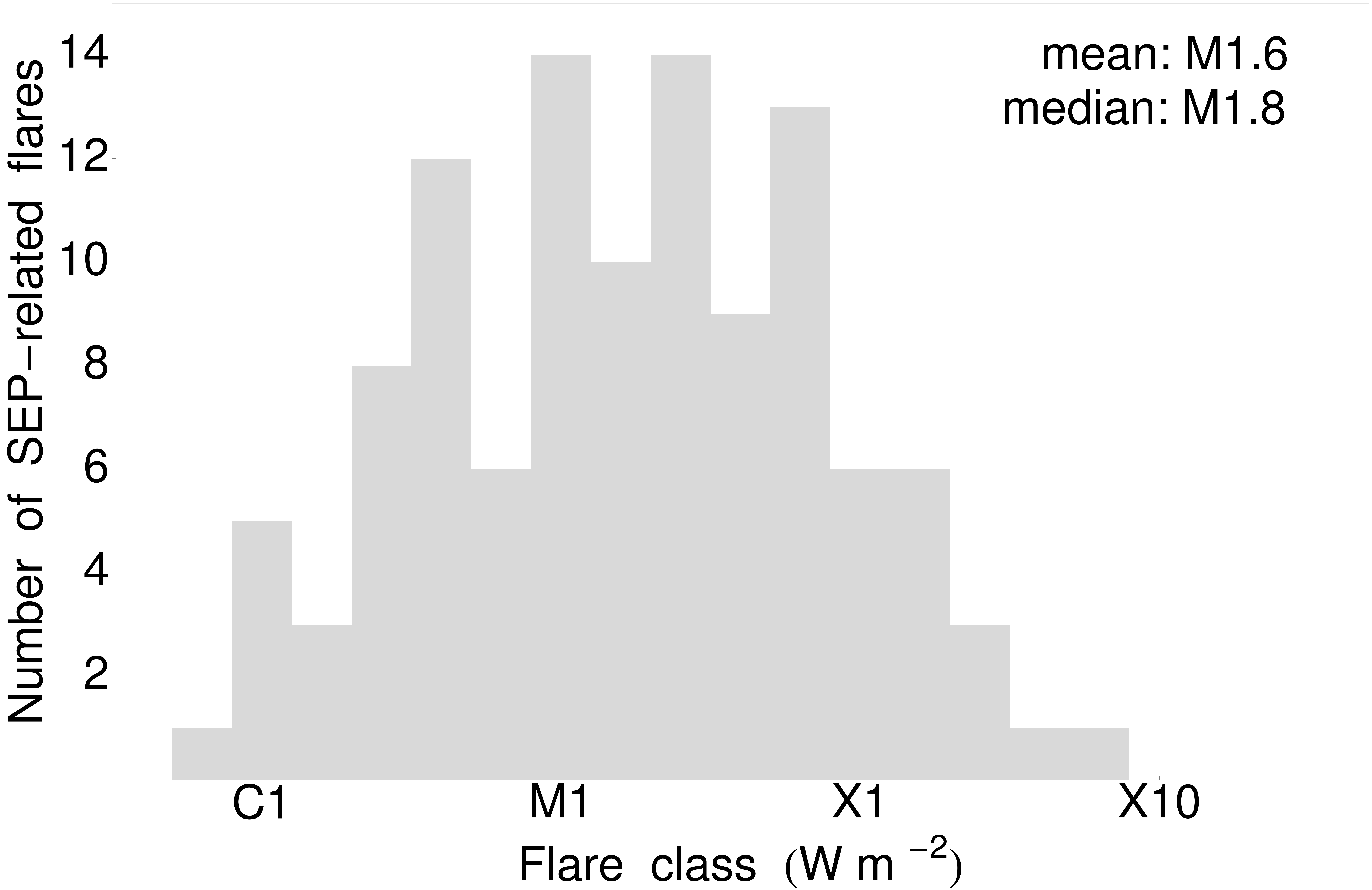
mean: M1.6
median: M1.8
Number of SEP−related flares
2
4
6
8
10
12
14
C1
M1
X1
X10
Flare class (W m $^{-2}$)

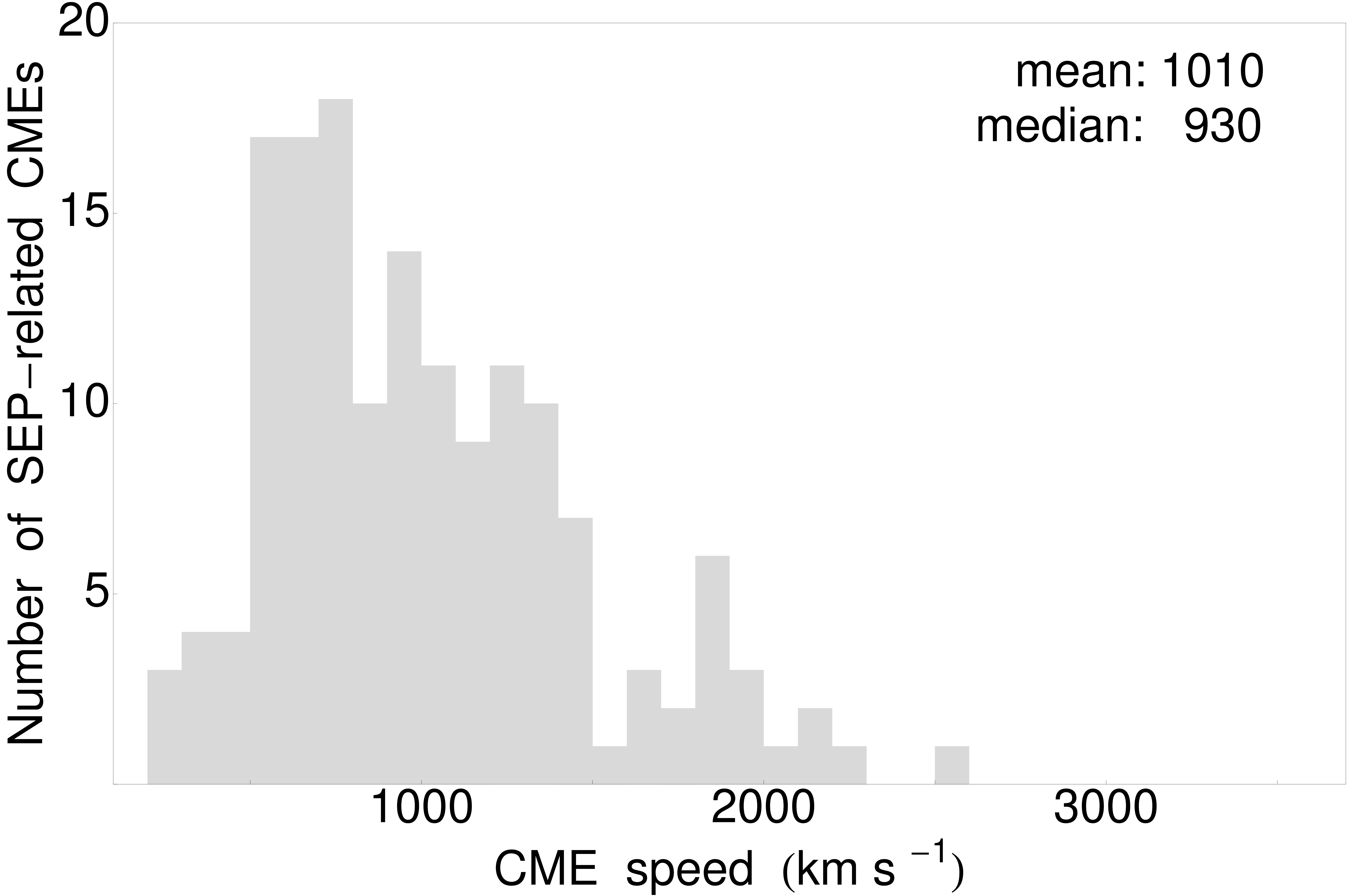
mean: 1010
median: 930
Number of SEP−related CMEs
20
15
10
5
1000
2000
3000
CME speed (km s −1)

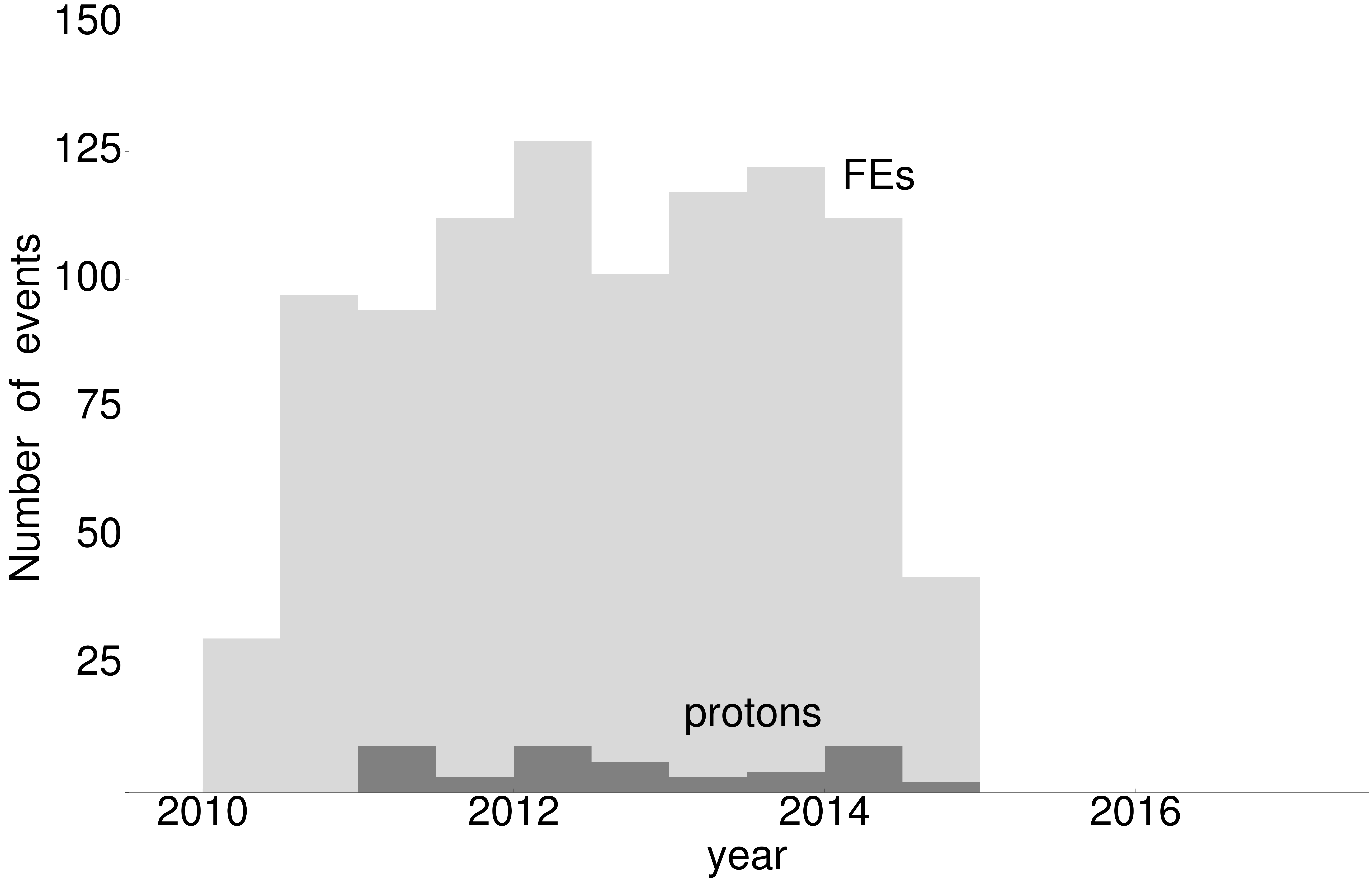
150
125
100
75
50
25
Number of events
FEs
protons
2010
2012
2014
2016
year

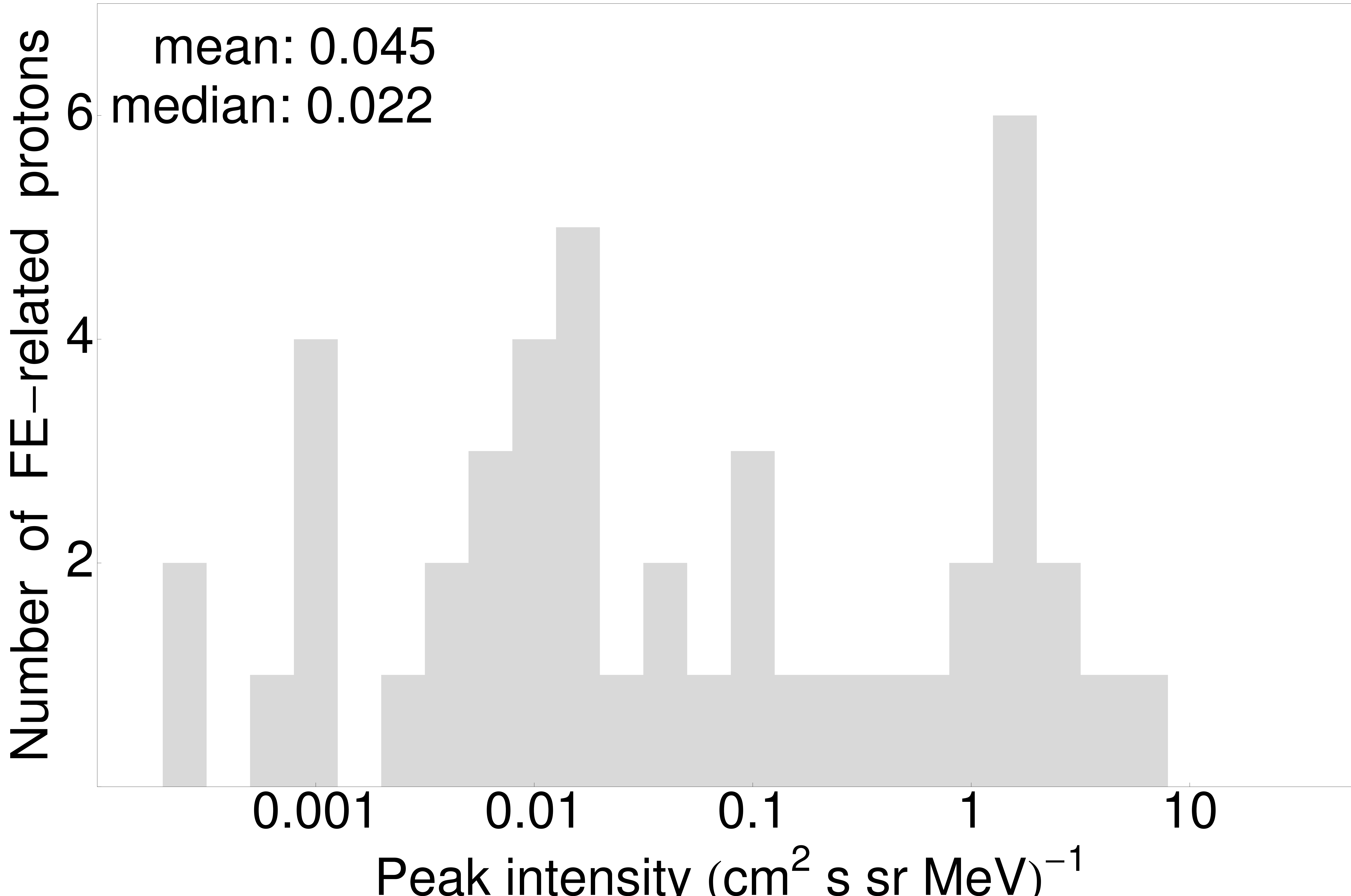
mean: 0.045
median: 0.022
Number of FE−related protons
6
4
2
0.001
0.01
0.1
1
10
Peak intensity (cm^2 s sr MeV)$^{-1}$

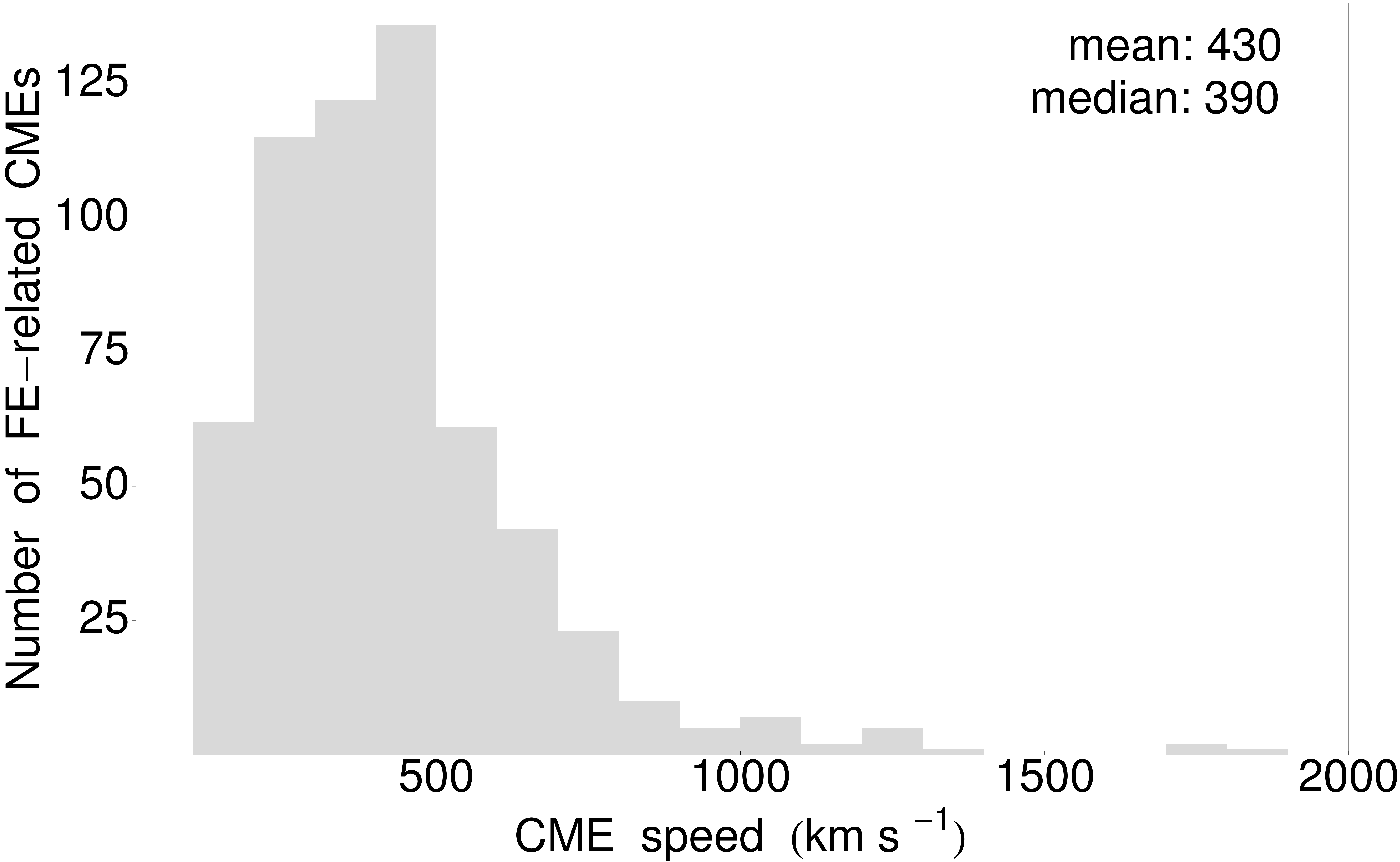
mean: 430
median: 390
Number of FE−related CMEs
125
100
75
50
25
500
1000
1500
2000
CME speed (km s −1)

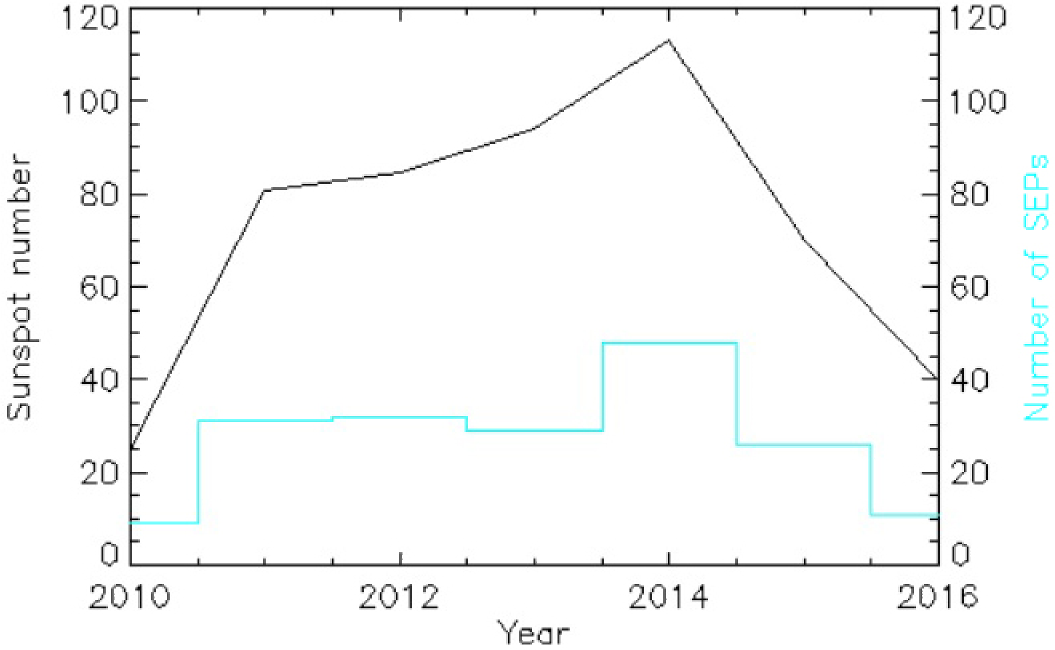

Sunspot number
Number of SEPs
Year
0
20
40
60
80
100
120
2010
2012
2014
2016

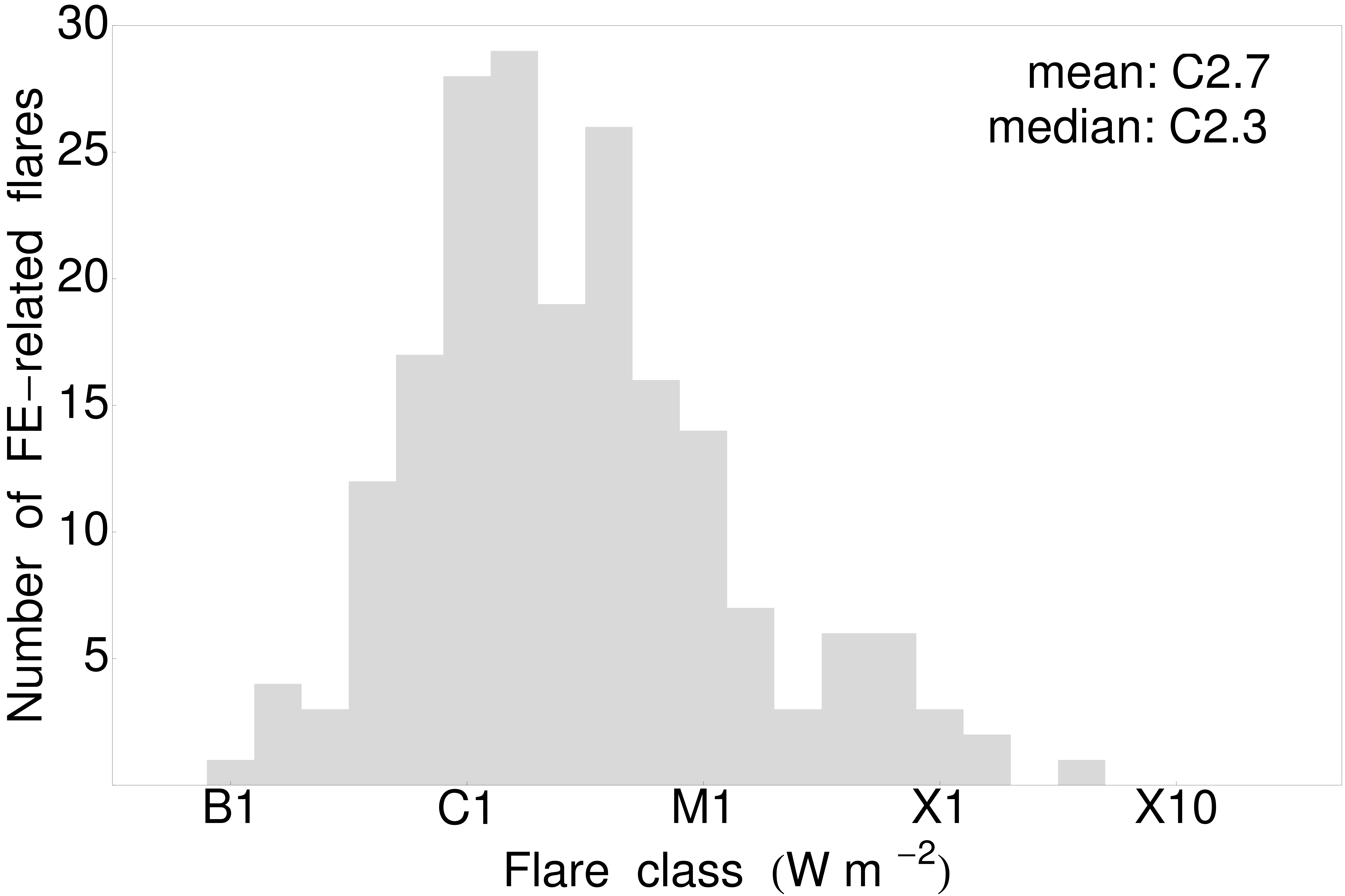

mean: C2.7
median: C2.3
Number of FE−related flares
30
25
20
15
10
5
B1
C1
M1
X1
X10
Flare class (W m −2)

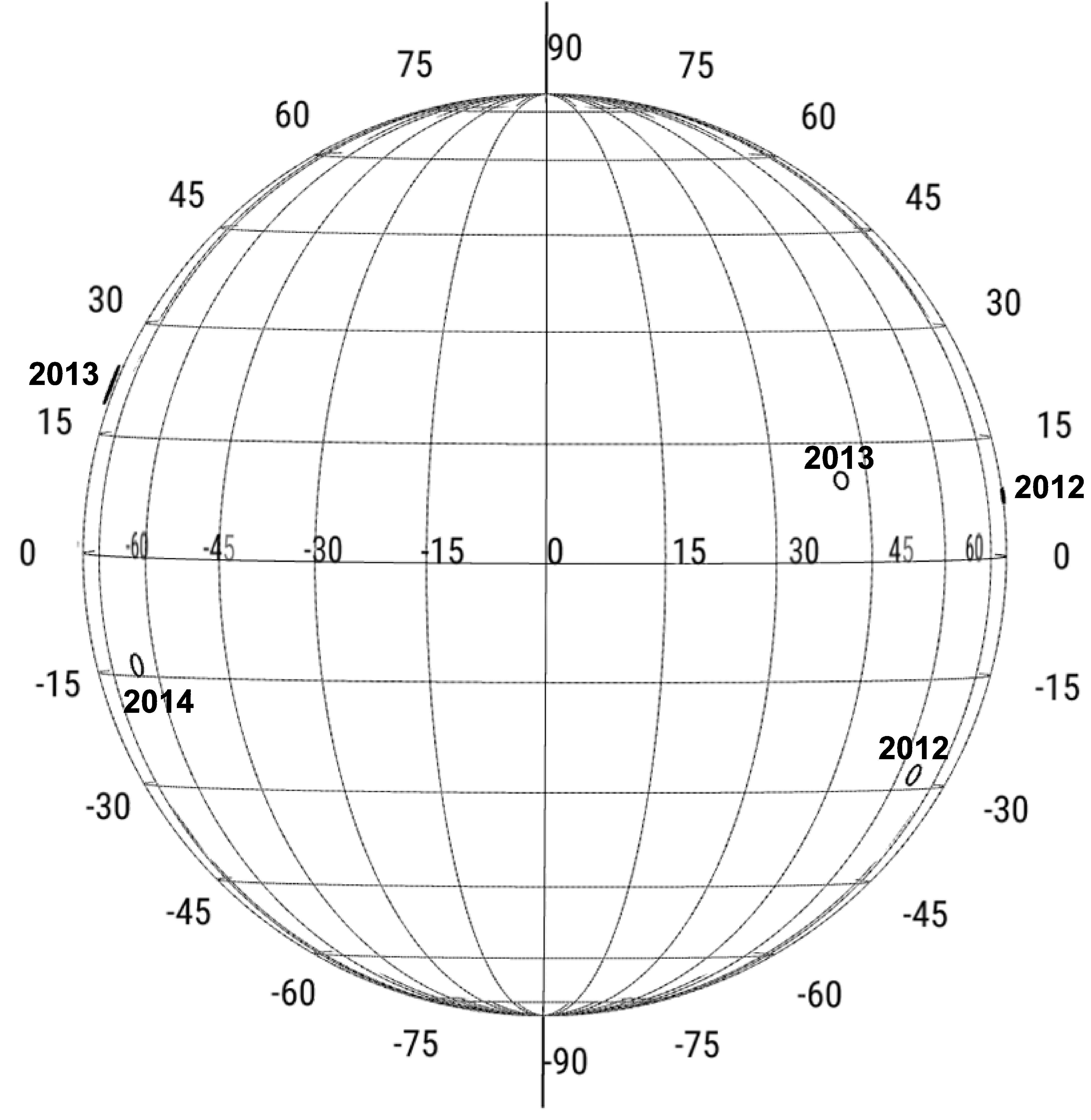
90
75
75
60
60
45
45
30
30
2013
15
15
2013
2012
0
-60
-45
-30
-15
0
15
30
45
60
0
-15
-15
2014
2012
-30
-30
-45
-45
-60
-60
-75
-75
-90